

## REFRACTION OF AN ELASTIC-PLASTIC SHOCK

W. LAKIN

Physics Department, Wichita State University, Wichita, Kansas 67208

**Abstract**—The refraction of an elastic-plastic shock incident at small angles on a material interface is studied theoretically. The basic flow is the multiple shock configuration describing regular reflection in fluid dynamics. Corrections to the basic flow satisfy first order perturbation equations, which are solved asymptotically.

### I. INTRODUCTION

PLANE shock waves are used to study some properties of materials at megabar pressures [1]. A preliminary theoretical study of the reflection and refraction of megabar shocks by material interfaces seems useful. The phenomena have been studied theoretically for elastic solids [2, 3]. The present study applies to solids unable to support shear stresses of the same order of magnitude as the compressional stress. For some problems, the shear stresses can be neglected, and an ideal fluid model is used. The theory of the reflection and refraction at an interface between ideal fluids is a special case of the theory of shock interactions [4, 5]. Problems involving regular reflection in gases have been solved numerically [6], and corresponding problems involving both gases and condensed matter have been solved graphically using shock polars [7-10]. The flows derived from ideal fluid models are called basic flows.

Superficially, it seems that small shear stresses can produce significant modifications of the basic flow because the latter contains a tangential discontinuity. The basic flow pattern, shown in Fig. 1, consists of five wedge-shaped constant state regions bounded by five half-planes originating at a common singular line. The half-planes  $i$ ,  $r$ ,  $t$ ,  $m$  and  $m'$  denote the incident shock front, reflected front, transmitted front, unshocked material interface, and shocked interface, respectively. Regions 4 and 5 contain unshocked material ahead of the incident and transmitted fronts, respectively. Regions 1, 2 and 3 contain material behind the transmitted, reflected and incident fronts, respectively. Flows in which the reflected shock is replaced by a rarefaction are not studied. The state is steady in an Eulerian coordinate system moving with the singular line. The shocked interface is usually a tangential discontinuity. Results obtained from theories which neglect shear stresses are often poor approximations to physical reality near tangential discontinuities. In special cases, the modification of the basic flow due to shear stresses can be obtained by perturbation theory. One of the special cases, the reflection and refraction of plane shocks incident at small angles upon a plane material interface, is the object of the present study.

The basic flow can be described more completely by considering the fluid dynamical counterpart. The five constant states manifestly satisfy the differential equations. The Rankine-Hugoniot equations are satisfied at all unperturbed shock fronts. Since the boundary conditions at the unshocked material interface are trivially satisfied, the only conditions the basic flow fails to satisfy are the boundary conditions at the shocked

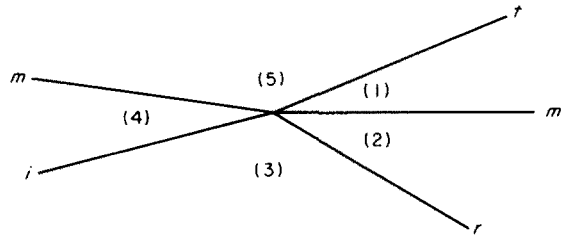


FIG. 1.  $m$ , Unshocked material interface.  $i$ , Incident shock front.  $t$ , Transmitted shock front.  $r$ , Reflected shock front.  $m'$ , Shocked material interface.

interface. The interface conditions may be regarded as four independent conditions; the continuity of normal and tangential components of velocity, and the vanishing of the two components of total force on the interface. The basic flow actually satisfies the two interface conditions involving normal components of vectors. The failure to satisfy the interface conditions on the tangential components of the vectors generates perturbations.

Section II contains a description of the relevant material properties. The critical problem is the description of plastic deformation, which limits the magnitude of the shear stresses. A simple macroscopic model of plastic flow is employed. The difference between the physical mechanism of plastic deformation and the model process limits the validity of the calculation. Alternative macroscopic theories may increase the complexity without significant improvement [11], and dislocation theories of dynamic plasticity are incomplete as well as complicated. Irreversible processes not characteristic of plastic flow are neglected. The differential equations describing the perturbed flow and the boundary conditions are derived in Section III. The perturbations are confined to regions one and two, and the perturbed boundaries are the reflected and transmitted fronts and the shocked interface. Realistic boundary conditions at the shocked interface may be partially unknown. The boundary conditions at the shock fronts are as reliable as the differential equations. Asymptotic solutions, valid at large distances from the singular line, are derived in Section IV. The approximation is similar to the boundary layer approximation of fluid dynamics. The asymptotic solutions exhibit the dependence of the results upon input parameters explicitly.

## II. MATERIAL PROPERTIES

The problem determines the model of the material and the properties derived from it. The basic flow is assumed to be described adequately by a fluid dynamical model. Since crystal imperfections determine stress relaxation, an elaborate model is required for a fundamental theory of the perturbations. The material is assumed to consist of regions of "good crystal" and "bad crystal" [12]. The "good crystal" is described by an isotropic elastic medium model. The only significant effect of the "bad crystal" is to provide a means of decay for some "good crystal" stresses. Since the process is treated crudely for reasons stated in the introduction, a description of the "bad crystal" state is not needed.

The elastic energy of the "good crystal" is a function of the six components of the elastic strain tensor and one additional thermodynamic quantity, such as the specific entropy. If the magnitudes of the elastic shear strains are much less than the magnitude of

the compressional strain, the problem can be partially linearized by using new variables instead of the elastic strains to describe the state of the "good crystal". In principle, the state at each point is described by a statistical ensemble of unit cells, but a representative unit cell with modified elastic moduli is adequate. A reference unit cell is chosen, and the transformation which maps the reference unit cell on the representative unit cell determines the elastic strains. If  $x_i$  is the  $i$ th coordinate of a point embedded in the representative unit cell and  $\mathbf{a}$  the position vector of the corresponding point in the reference unit cell, the transformation is specified by representing  $x_i$  as a function of  $\mathbf{a}$  and time  $t$ . For infinitesimal time intervals, the description of motion is equivalent to the Lagrangian kinematics of continuous media [4, 5]. Since the transformation must have an inverse, all kinematic quantities can be expressed as functions of Eulerian coordinates.

It is convenient to start with a notation adapted to the problem of interest. Symbols and equations with numerical subscripts 1 or 2 refer to the indicated region of Fig. 1, while symbols without subscripts refer to either region. Symbols without superscripts denote basic flow quantities, primed symbols denote perturbations, and asterisks denote total quantities. The deformation gradients  $\Gamma_{ij}^*$  are defined to be

$$\Gamma_{ij}^* = \left( \frac{\partial x_i}{\partial a_j} \right)_L. \quad (2.1)$$

The subscript  $L$  indicates differentiation in which  $t$  and components of  $\mathbf{a}$  are the independent variables. The nine  $\Gamma_{ij}^*$  form a  $3 \times 3$  matrix, denoted by  $\Gamma^*$ . The components of the macroscopic flow velocity vector  $\mathbf{v}^*$  are

$$\mathbf{v}_i^* = \left( \frac{\partial x_i}{\partial t} \right)_L. \quad (2.2)$$

The vector defined by equation (2.2) must not be confused with the microscopic flow velocity. If a macroscopic sample of material is instantaneously deformed homogeneously and then held in the deformed state, the "good crystal" state may change by plastic deformation. The process requires microscopic flow, but the macroscopic flow velocity vanishes. A theory describing the microscopic flow velocity is essentially a microscopic theory of dynamic plasticity, which is not considered.

The matrix  $\Gamma^*$  may be expressed as a product of a symmetric matrix  $\Gamma^{s*}$  and a rotation matrix  $\Gamma^{r*}$  [13]. Finally  $\Gamma^{s*}$  is expressed as a product of a positive number  $\Lambda^*$  and a symmetric unimodular matrix  $\Gamma^{h*}$ .

$$\Gamma^* = \Lambda^* \Gamma^{h*} \Gamma^{r*}. \quad (2.3)$$

The ratio of the respective volumes of the representative and reference unit cells equals  $\Lambda^{*3}$ . An approximation with a wide range of applications is that  $\Gamma^{h*}$  differs slightly from the identity.

$$\Gamma_{ij}^{h*} = \delta_{ij} + h_{ij}^*. \quad (2.4)$$

The elements of  $h^*$  are small and quantities of second order in the elements of  $h^*$  are neglected. The requirement that  $\Gamma^{h*}$  be unimodular implies that the trace of  $h^*$  vanishes to first order. Any five independent elements of  $h^*$ , together with the density, can replace the elastic strains as "good crystal" state variables.

The set of flow equations must contain equations describing the rate of change of the independent elements of  $h^*$ . The needed equations are derived from equations describing

the rate of change of  $\Gamma^*$ . Two processes contribute to the rate of change of  $\Gamma^*$ , the inhomogeneity of the macroscopic flow velocity and plastic flow. The effect of inhomogeneity of the macroscopic flow is calculated directly in Appendix I. The result is

$$\left(\frac{\partial h_{ij}^*}{\partial t}\right)_L = \frac{1}{2}(\nabla_i v_j^* + \nabla_j v_i^*) - \frac{1}{3}\delta_{ij}\nabla \cdot \mathbf{v}^*. \tag{2.5}$$

The symbol  $\nabla_i$  denotes a derivative with respect to  $x_i$  with Eulerian coordinates and time as independent variables. Plastic flow generally produces no significant changes in density or spatial orientation. Formally, the change in  $\Gamma^*$  is due to changes in  $h^*$ . The rate of change of  $h^*$  must transform like  $h^*$ , be symmetric, and have trace equal to zero; but diverse possibilities remain. If the basic flow is described by a fluid model, a useful assumption may be

$$\left(\frac{\partial h'_{ij}}{\partial t}\right)_P = -\lambda h'_{ij}. \tag{2.6}$$

The subscript  $P$  indicates the change due to plastic flow, and the time  $t$  and components of  $\mathbf{a}$  are the independent variables. Equation (2.6) implies the relaxation of shear strains does not involve diffusion. The parameter  $\lambda$  is positive and constant in each region of Fig. 1, but need not be determined by the density and specific entropy. The shock front ahead of the region is part of the stress history of the material, and  $\lambda$  may be drastically influenced by the structure of the front.

The “good crystal” properties are determined by the functional dependence of  $E^*$ , the specific internal energy, upon density  $\rho^*$ , specific entropy  $S^*$ , and the elements of  $h^*$ .

$$E^* = E_g^* + C_t^{*2} \sum_{ij} h_{ij}^{*2} \tag{2.7}$$

In equation (2.12),  $E_g^*$  is a Mie–Grueneisen approximation to the specific internal energy, and  $C_t^*$  is a function of  $\rho^*$  and  $S^*$  equal to the speed of infinitesimal transverse waves. The pressure  $P^*$  is

$$P^* = \rho^{*2} \frac{\partial E_g^*}{\partial \rho^*}. \tag{2.8}$$

### III. FIRST ORDER EQUATIONS

The equations of motion in Eulerian coordinates differ from their fluid dynamical counterparts only in the equation of state and stress tensor. The standard equations are

$$\frac{\partial \rho^*}{\partial t} + \mathbf{v}^* \cdot \nabla \rho^* = -\rho^* \nabla \cdot \mathbf{v}^* \tag{3.1}$$

$$\rho^* \left( \frac{\partial v_i^*}{\partial t} + \mathbf{v}^* \cdot \nabla v_i^* \right) = \sum_j \nabla_j \sigma_{ij}^* \tag{3.2}$$

$$\rho^* \left( \frac{\partial E^*}{\partial t} + \mathbf{v}^* \cdot \nabla E^* \right) = \sum_{ij} (\nabla_i v_j^*) \sigma_{ij}^*. \tag{3.3}$$

The symbol  $\sigma_{ij}^*$  denotes the elastic stress tensor. Equations (3.1), (3.2) and (3.3) are generally called the conservation equations for mass, momentum and energy respectively. The stress

tensor satisfies

$$\sigma_{ij}^* = -P^* \delta_{ij} + 2\rho^* C_t^{*2} h_{ij}^*. \tag{3.4}$$

Equation (3.4) is derived in Appendix II. The time derivatives in equations (3.1)–(3.3) vanish if the flow is steady. Linearized equations are obtained by expressing quantities in the form

$$\rho^* = \rho + \rho', \tag{3.5}$$

inserting into equations (3.1)–(3.3), and retaining first order terms only. Space derivatives of basic flow quantities vanish.

$$\mathbf{v} \cdot \nabla \rho' = -\rho \nabla \cdot \mathbf{v}', \tag{3.6}$$

$$\rho \mathbf{v} \cdot \nabla v'_i = -\nabla_i P' + 2\rho C_t^2 \sum_j \nabla_j h'_{ij}, \tag{3.7}$$

$$\rho \mathbf{v} \cdot \nabla E' = -P \nabla \cdot \mathbf{v}'. \tag{3.8}$$

Equation (3.8) transforms into

$$\mathbf{v} \cdot \nabla S' = 0. \tag{3.9}$$

Equations (3.9) and (3.6) yield

$$\mathbf{v} \cdot \nabla P' = -\rho C_g^2 \nabla \cdot \mathbf{v}'. \tag{3.10}$$

Equations (3.9) and (3.10) are derived in Appendix III. Here  $C_g$  is the speed of sound in the Mie–Grüneisen approximation. Since the elements of  $h$  vanish, first order equations are obtained by adding the right sides of equations (2.5) and (2.6).

$$\mathbf{v} \cdot \nabla h'_{ij} = \frac{1}{2}(\nabla_i v'_j + \nabla_j v'_i) - \frac{1}{3} \delta_{ij} \nabla \cdot \mathbf{v}' - \lambda h'_{ij}. \tag{3.11}$$

Equations (3.7) and (3.9)–(3.11) are a complete set of first order equations.

Since the elements of  $h$  vanish, the Rankine–Hugoniot Equations are a complete set of boundary or jump conditions at the shock fronts. It is convenient to use special coordinates, denoted by  $(r, s)$ . The coordinate  $r$  is the displacement along the unperturbed front, and  $s$  is the perpendicular displacement in the direction of the material flow. The perturbation of the front is described by a function  $s_f(r)$ , a first order quantity. The approximate unit normal is

$$\mathbf{n}^* = \mathbf{e}_s - \frac{ds_f}{dr} \mathbf{e}_r. \tag{3.12}$$

The bold faced  $\mathbf{e}$  with subscripts denotes a unit vector. The corresponding approximate unit tangent to the perturbed front is

$$\mathbf{e}^* = \mathbf{e}_r + \frac{ds_f}{dr} \mathbf{e}_s. \tag{3.13}$$

The Rankine–Hugoniot Equations are

$$J^* = \rho^* \mathbf{v}^* \cdot \mathbf{n}^* = \rho^A \mathbf{v}^A \cdot \mathbf{n}^* \tag{3.14}$$

$$J^*(\mathbf{v}^* - \mathbf{v}^A) \cdot \mathbf{n}^* = \sum_{ij} (\sigma_{ij}^* - \sigma_{ij}^A) n_i^* n_j^* \tag{3.15}$$

$$J^*(\mathbf{v}^* - \mathbf{v}^A) \cdot \mathbf{e}^* = \sum_{ij} (\sigma_{ij}^* - \sigma_{ij}^A) n_i^* e_j^* \tag{3.16}$$

$$J^*(E^* + \frac{1}{2} v^{*2} - E^A - \frac{1}{2} v^{A2}) = \sum_{ij} (\sigma_{ij}^* v_i^* - v_{ij}^A v_{ij}^A) n_j^*. \tag{3.17}$$

Equations (3.14)–(3.17) describe the conservation of mass, the change in the normal component of momentum, the change in the tangential component of momentum, and the change in total energy respectively. The symbol  $J^*$  denotes the rate of flow of mass across unit area of shock front, the superscript  $A$  refers to unperturbed regions upstream from the shock front, and subscripts  $i$  and  $j$  denote Cartesian components of the vectors. Equations (3.14) and (3.17) are linearized, and the results are

$$\mathbf{v} \cdot \mathbf{e}_s \rho' + \rho \mathbf{v}' \cdot \mathbf{e}_s - \rho(1 - \varepsilon) \mathbf{v} \cdot \mathbf{e}_r \frac{ds_f}{dr} = 0 \tag{3.18}$$

$$P' - 2\rho C_t^2 \sum_{ij} h'_{ij} e_{si} e_{sj} + J \mathbf{v}' \cdot \mathbf{e}_s + J(1 - \varepsilon) \mathbf{v} \cdot \mathbf{e}_r \frac{ds_f}{dr} = 0 \tag{3.19}$$

$$-2\rho C_t^2 \sum_{ij} h'_{ij} e_{si} e_{rj} + J \mathbf{v}' \cdot \mathbf{e}_r + J \frac{1 - \varepsilon}{\varepsilon} \mathbf{v} \cdot \mathbf{e}_s \frac{ds_f}{dr} = 0 \tag{3.20}$$

$$\rho T S' + P' - 2\rho C_t^2 (\mathbf{v} \cdot \mathbf{e}_s)^{-1} \sum_{ij} h'_{ij} v_i e_{sj} + \rho \mathbf{v} \cdot \mathbf{v}' = 0 \tag{3.21}$$

$$\varepsilon = \rho^A / \rho. \tag{3.22}$$

The derivation of equation (3.21) in greater detail is in Appendix IV. The temperature is denoted by  $T$ , and  $e_{si}$  and  $e_{ri}$  denote the  $i$ th component of  $\mathbf{e}_s$  and  $\mathbf{e}_r$ , respectively. As shown in Appendix IV, equation (3.18) can be replaced by

$$\frac{1}{\rho} \left( \frac{\partial \rho}{\partial S} \right)_P J S' + \frac{J}{\rho C_g^2} P' + \rho \mathbf{v}' \cdot \mathbf{e}_s - \rho(1 - \varepsilon) \mathbf{v} \cdot \mathbf{e}_r \frac{ds_f}{dr} = 0. \tag{3.23}$$

Equations (3.19)–(3.23) form a complete set of first order boundary conditions at the unperturbed shock fronts.

The boundary conditions at the shocked interface may be more diverse than the jump conditions at shock fronts. The generally valid conditions are the velocity is tangential to the interface and the forces on the interface exerted by the two materials cancel. If fracture at the interface does not occur, the material velocity is continuous. If surface energies can be neglected, the forces on the interface are obtained from equation (3.4). The neglect of both fracture and surface energies is not expected to be valid often, but constitutes a useful approximation at the outset. An advantage of the asymptotic method is the explicit formulae for the solutions are easily modified to account for changes in boundary conditions.

It is convenient to choose the singular line as  $z$ -axis and the intersection of the unperturbed shocked interface with the  $xy$ -plane as the  $x$ -axis. The shocked interface is described by a function  $y_I(x)$ , also a first order quantity. The approximate units normal and tangent are respectively

$$\mathbf{n}^* = \mathbf{e}_y - \frac{dy_I}{dx} \mathbf{e}_x \tag{3.24}$$

$$\mathbf{e}^* = \mathbf{e}_x + \frac{dy_I}{dx} \mathbf{e}_y. \tag{3.25}$$

Continuity of tangential and normal components of velocity across the interface implies

$$(\mathbf{v}_1^* - \mathbf{v}_2^*) \cdot \mathbf{e}^* = 0 \tag{3.26}$$

$$(\mathbf{v}_1^* - \mathbf{v}_2^*) \cdot \mathbf{n}^* = 0. \tag{3.27}$$

The vanishing of the two components of total force on the interface implies

$$\sum_{ij} (\sigma_{1ij}^* - \sigma_{2ij}^*) n_i^* n_j^* = 0 \tag{3.28}$$

$$\sum_{ij} (\sigma_{1ij}^* - \sigma_{2ij}^*) n_i^* e_j^* = 0. \tag{3.29}$$

The unperturbed vectors  $\mathbf{v}_1$  and  $\mathbf{v}_2$  are parallel to the  $x$ -axis, and the difference between the magnitudes  $v_1$  and  $v_2$  is a first order quantity because the angle of incidence is small. Equations (3.26)–(3.29) are linearized to obtain

$$v'_{1x} - v'_{2x} = -w; \quad w = v_1 - v_2 \tag{3.30}$$

$$v'_{1y} - v'_{2y} = 0. \tag{3.31}$$

$$-P'_1 + 2\rho_1 C_{i1}^2 h'_{1yy} + P'_2 - 2\rho_2 C_{i2}^2 h'_{2yy} = 0 \tag{3.32}$$

$$2\rho_1 C_{i1}^2 h'_{1xy} - 2\rho_2 C_{i2}^2 h'_{2xy} = 0. \tag{3.33}$$

Equations (3.30)–(3.34) are a complete set of boundary conditions at the unperturbed shocked interface. The function  $y_I(x)$  can be determined from the conditions that the component of velocity normal to the interface vanishes.

$$\mathbf{v}_1 \cdot \mathbf{n}^* = 0. \tag{3.34}$$

The linearized form is

$$v'_{1y} - \bar{v} \frac{dy_I}{dx} = 0; \quad \bar{v} = \frac{1}{2}(v_1 + v_2) \tag{3.35}$$

$$\frac{dy_I}{dx} = \frac{1}{\bar{v}} v'_{1y} = \frac{1}{\bar{v}} v'_{2y}. \tag{3.36}$$

#### IV. ASYMPTOTIC SOLUTIONS

Equations (3.7), (3.9)–(3.11) are transformed into uncoupled equations by means of vector and scalar potentials

$$\mathbf{v}' = \nabla\psi \times \mathbf{e}_z + \nabla\varphi. \tag{4.1}$$

The uncoupled equations are

$$\alpha_i^2 \frac{\partial^2 \psi}{\partial x^2} - \frac{\partial^2 \psi}{\partial y^2} + \alpha_i \frac{\partial \psi}{\partial x} = 0 \tag{4.2}$$

$$\alpha_i^2 \frac{\partial^2 \varphi}{\partial x^3} - \frac{\partial^3 \varphi}{\partial x \partial y^2} + \alpha_i \left( \alpha_g^2 \frac{\partial^2 \varphi}{\partial x^2} - \frac{\partial^2 \varphi}{\partial y^2} \right) = 0 \tag{4.3}$$

$$C_i^2 = C_g^2 + \frac{4}{3} C_i^2 \tag{4.4}$$

$$\alpha_l^2 = \frac{v^2}{C_l^2} - 1; \quad \alpha_g^2 = \frac{v^2}{C_g^2} - 1; \quad \alpha_t^2 = \frac{v^2}{C_t^2} - 1 \tag{4.5}$$

$$\kappa_l = \frac{\lambda}{v} \frac{C_g^2}{C_l^2}; \quad \kappa_t = \frac{\lambda v}{C_t^2} \tag{4.6}$$

The quantity denoted by  $C_l$  equals the speed of infinitesimal longitudinal waves.

Integral representations of solutions of equation (4.3) are obtained by assuming the  $x$ -dependence can be represented as a Fourier integral in the complex plane. Two solutions of equation (4.3) are

$$\varphi^{(\pm)} = \int_{(R+)} \Phi^{(\pm)} e^{i(kx \pm \alpha_g m |y|)} dk \tag{4.7}$$

$$m = kM; \quad M = \sqrt{\left| \frac{k - i\kappa_l'}{k - i\kappa_l} \right|} \tag{4.8}$$

$$\kappa_l' = \frac{\alpha_g^2}{\alpha_l^2} \kappa_l = \frac{\lambda}{v} \sqrt{\left| \frac{v^2 - C_g^2}{v^2 - C_l^2} \right|} \tag{4.9}$$

The contour  $(R+)$  follows the real axis of the  $k$ -plane and goes around the origin in the positive direction. The branch points are on the positive imaginary axis, and the cut is the straight line segment joining them. At large  $|k|$ ,  $M$  approximately equals unity. The two functions of equation (4.7) added produce  $\varphi$ , and the functions  $\Phi^{(\pm)}(k)$  are determined by the boundary conditions.

Integral representations of solutions of equation (4.2) also exist. One solution is analogous to the above solutions of equation (4.3)

$$\psi^{(-)} = \int_{(R+)} \Psi^{(-)} e^{ikx - n|y|} dk \tag{4.10}$$

$$n = \sqrt{(\kappa_t k i - \alpha_t^2 k^2)} \tag{4.11}$$

The branch points of  $n$  are at the origin and on the positive imaginary axis of the  $k$ -plane. The integral with the opposite sign of  $n$  in equation (4.10) diverges in the physical domain. A useful second solution is

$$\psi^{(+)} = \int_{I(+)} \Psi^{(+)} e^{ikr - qs} dk \tag{4.12}$$

$$q = \frac{1}{\beta_l^2 - 1} \{ [\frac{1}{2} \kappa_t + (\alpha_t^2 + 1)(ik) \cos \theta] |\sin \theta| + \sqrt{[\frac{1}{4} \kappa_t^2 \sin^2 \theta + \kappa_t(ik) \cos \theta - \alpha_t^2 k^2]} \} \tag{4.13}$$

$$\beta_l = \frac{v}{C_l} |\sin \theta|; \quad \beta_g = \frac{v}{C_g} |\sin \theta|; \quad \beta_t = \frac{v}{C_t} |\sin \theta| \tag{4.14}$$

The angles between the unperturbed fronts and the unperturbed interface are denoted by  $\theta$ . The angle  $\theta_1$  is positive and  $\theta_2$  is negative. The branch points of  $q$  are in the upper half of the  $k$ -plane. If the component of velocity normal to the unperturbed front is greater than  $C_l$  ( $\beta_l > 1$ ), the branch points are symmetrical with respect to the imaginary axis. The cut joins the branch points, is parallel to the real axis, and passes through infinity. The radical of equation (4.13) is positive at the origin. The contour  $(I+)$  encircles the

positive imaginary axis in the positive direction. All singularities of the integrand not on the positive imaginary axis are outside of  $(I+)$ .

Each potential is the sum of the two independent solutions represented by the above integrals. The coefficient functions,  $\Phi^{(\pm)}(k)$  and  $\Psi^{(\pm)}(k)$ , are determined by boundary conditions. The evaluation of the coefficients depends on the solution of coupled integral equations of the first kind. If a solution which only satisfies the boundary conditions asymptotically is acceptable, the problem is reduced to the solution of algebraic equations. The coefficients must be singular at  $k$  equals zero because the right side of equation (3.30) is independent of  $x$ , but the coefficients can be analytical below  $(R+)$ . If  $\beta_i > 1$ , the integral in equation (4.10) can be closed by a large semicircle in the lower half of the  $k$ -plane when  $(x, y)$  represents a point on the unperturbed front. The potential  $\psi^{(-)}$  vanishes on the front.

The asymptotic values of the functions specified by equations (4.7), (4.10) and (4.12) are determined by the values of the integrands at small  $k$ . In equation (4.7), the quantity denoted by  $m$  is replaced by  $k$  ( $\alpha_i/\alpha_g$ ). The factor  $(x - \alpha_g|y|)$  in the exponential is negative if the component of velocity normal to the unperturbed front is greater than the Grueneisen sound speed, an improbable situation. Should this occur, the usual stability argument [5] suggests the unperturbed shock is unstable against disturbances with sufficiently small wave numbers. The problem is restricted to the case where  $\beta_g < 1$ . Integral representations for components of  $v'$ ,  $P'$ , and elements of  $h'$  are obtained from equations (4.1), (3.10) and (3.11) respectively. Approximate forms of the Fourier coefficients are

$$\Phi^{(\pm)} = A^{(\pm)} \left( \frac{1}{ki} \right)^a \quad (4.15)$$

$$\Psi^{(+)} = \tau A \left( \frac{1}{ki} \right)^b \quad (4.16)$$

$$\Psi^{(-)} = \tau B \left( \frac{1}{ki} \right)^d \quad (4.17)$$

The constants  $a$ ,  $b$ ,  $d$ ,  $A^{(\pm)}$ ,  $A$  and  $B$  are determined by the boundary conditions, and  $\tau$  equals  $(+1)$  in region 1 and  $(-1)$  in region 2.

The boundary conditions at the unperturbed shock front yield the results that  $b$  equals  $a$  and relations among the  $A$ 's.

$$A^{(+)} = HA^{(-)}; \quad A = KA^{(-)}. \quad (4.18)$$

Approximations to  $H$  and  $K$  are in Table 1. They are correct to lowest order in  $\theta$  if all  $\beta$ 's defined in equations (4.14) are large compared to  $|\theta|$ . Since the asymptotic values of quantities are determined by the small  $|k|$  terms in the integral representations, the interface conditions separate into two pairs. Equations (3.30) and (3.33), which involve tangential components of velocity and force, yield the value of  $d$  and two simultaneous equations determining  $B_1$  and  $B_2$ . Equations (3.31) and (3.32) yield the value of  $a$  and two equations determining  $A_1^{(-)}$  and  $A_2^{(-)}$  in terms of  $B_1$  and  $B_2$ . The values of the constants in equations (4.15)–(4.18), approximated to leading order in  $|\theta|$ , are in Table 1. Physical quantities are obtained by asymptotic evaluation of their contour integral representations.

TABLE I

Quantity	Value or formula
$a$	$3/2$
$b$	$3/2$
$d$	$3/2$
$H$	$-\sqrt{\frac{1-\beta_g}{1+\beta_g}}Q$
$K$	$\frac{2(1+\beta_g)\sqrt{(1-\beta_g)}}{R}$
$Q$	$\frac{(\alpha_g-1)F+(1-\beta_g)G}{R}$
$R$	$(\alpha_g+1)F+(1+\beta_g)G$
$F$	$\frac{\varepsilon}{1-\varepsilon} \frac{1}{ \sin \theta }$
$G$	$\frac{1+\gamma\beta_g^2}{\beta_g \sin^2 \theta}$
$\gamma$	$\frac{\rho}{T} \left( \frac{\partial T}{\partial \rho} \right)_s$
$B_1$	$\frac{w}{2\pi} \frac{\rho_2}{\rho_{12}} \frac{1}{\sqrt{\kappa_{12}}}$
$B_2$	$\frac{w}{2\pi} \frac{\rho_1}{\rho_{12}} \frac{1}{\sqrt{\kappa_{12}}}$
$A_1^{(-)}$	$D(1+H_2)B_1$
$A_2^{(-)}$	$D(1+H_1)B_2$
$\kappa_{12}$	$\kappa_{r1} + \kappa_{r2}$
$\rho_{12}$	$\frac{\rho_1\sqrt{\kappa_{r1}} + \rho_2\sqrt{\kappa_{r2}}}{\sqrt{\kappa_{12}}}$
$D$	$\frac{\rho_1 - \rho_2}{\alpha_{g1}(1-H_1)(1+H_2)\rho_2 + \alpha_{g2}(1-H_2)(1+H_1)\rho_1}$

It may be interesting to examine the dependence of various quantities on the parameters  $c_t$  and  $\lambda$ , which do not influence the basic flow. The dependence is determined by the coefficients  $B_1$  and  $B_2$ . The various  $A$ 's are equal to one of the  $B$ 's multiplied by factors independent of  $c_t$  or  $\lambda$ . Other parameters are determined by the Mie-Grueneisen equation of state. The dependence on  $c_t$  and  $\lambda$  is contained in the factor  $(1/\rho_{12}\sqrt{\kappa_{12}})$

$$\frac{1}{\rho_{12}\sqrt{\kappa_{12}}} = \frac{1}{\rho_1\sqrt{\kappa_{r1}} + \rho_2\sqrt{\kappa_{r2}}}. \quad (4.19)$$

The  $\kappa_r$ 's are defined by equation (4.6). In the asymptotic approximation,  $c_t$  is not determined independent of the model used to describe dynamic plasticity. A typical physical

quantity is the slope of the transmitted shock front.

$$\left(\frac{ds_f}{dr}\right)_1 = \xi \frac{\rho_1}{\rho_1 \sqrt{x_{t1}} + \rho_2 \sqrt{x_{t2}}} \frac{1}{\sqrt{(\pi r)}} \quad (4.20)$$

$$\xi = K_1(1 + H_2)D \frac{\varepsilon_1}{(1 - \varepsilon_1)^2} \frac{w}{\bar{v}}. \quad (4.21)$$

The parameter  $\xi$  is determined by the equation of state.

A comparison between the above calculation and boundary layer theory in ordinary fluid dynamics is interesting. Vortex flow in fluids is the counterpart of transverse waves in solids. In both approximations, the transverse waves contribute the leading terms of the physical quantities (not potentials) near the tangential discontinuity of the basic flow. The corrections are of order  $(L/x)^{\frac{1}{2}}$ , where  $L$  is a length defined by the relevant irreversible process. Boundaries other than the unperturbed tangential discontinuities do not influence the leading terms. The two approximations are related, but differ in the method of determining orders of magnitude of some terms. For example, in boundary layer theory, derivatives with respect to  $x$  are of higher order than derivatives with respect to  $y$  [14]. In the above approximation, this ordering applies only to terms obtained from  $\psi^{(-)}$ . The above approximation may have interesting analogues in other compressible flow problems.

## REFERENCES

- [1] R. G. MCQUEEN *et al.*, in *High-Velocity Impact Phenomena*. Edited by R. KINSLOW. Academic Press (1970).
- [2] T. W. WRIGHT, *Int. J. Solids Struct.* **7**, 161 (1971).
- [3] T. W. WRIGHT, *Arch. rationl. Mech. Analysis* **42**, 115 (1971).
- [4] R. COURANT and K. O. FRIEDRICKS, *Supersonic Flow and Shock Waves*. Interscience (1948).
- [5] L. D. LANDAU and E. M. LIFSHITZ, *Fluid Mechanics*. Pergamon Press (1959).
- [6] L. F. HENDERSON, *J. Fluid Mech.* **26**, 607 (1966).
- [7] A. K. OPPENHEIM, J. J. SMOLEN and L. J. ZAJAE, *Comb. Flame* **12**, 63 (1968).
- [8] A. K. OPPENHEIM, J. J. SMOLEN, D. KWAK and P. URTIEW, in *Fifth International Symposium in Detonations*.
- [9] P. LAHARRAGUE, J. MOWAN and J. THOUVENIN, in *Proc. Symposium on Behaviour of Dense Media under High Dynamic Pressure*, p. 153, Dunod, Paris (1968).
- [10] T. J. AHRENS and P. A. URTIEW, UCRL-51109 (TID-4500, UC-34, Physics), Lawrence Livermore Laboratory, Livermore, California (1971).
- [11] A. K. HEAD, in *Inelastic Behavior of Solids*. Edited by M. F. KANNINEN *et al.* McGraw-Hill (1970).
- [12] F. D. FRANK, *Phil. Mag.* **42**, 809 (1951).
- [13] J. R. RICE, *J. Mech. Physics Solids* **19**, 433 (1971).
- [14] N. CURLE, *The Laminar Boundary Layer Equations*. Clarendon Press (1962).

## APPENDIX I

The time derivative of equation (2.1) is combined with equation (2.2) to obtain

$$\left(\frac{\partial \Gamma_{ij}^*}{\partial t}\right)_i = \left(\frac{\partial v_i^*}{\partial a_j}\right)_i = \sum_k (\nabla_k v_i^*) \Gamma_{kj}^*. \quad (I.1)$$

If  $\Delta^*$  is the matrix with  $ij$ -element equal to  $(\nabla_j v_i^*)$ ,

$$\left(\frac{\partial \Gamma^*}{\partial t}\right)_L = \Delta^* \Gamma^*. \quad (I.2)$$

The left side of equation (I.2) is obtained from equations (2.3) and (2.4)

$$\left(\frac{\partial \Gamma^*}{\partial t}\right)_L = \left(\frac{\partial \Lambda^*}{\partial t}\right)_L \Gamma^{h*} \Gamma^{r*} + \Lambda^* \left(\frac{\partial h^*}{\partial t}\right) \Gamma^{r*} + \Lambda^* \Gamma^{h*} \left(\frac{\partial \Gamma^{r*}}{\partial t}\right)_L \tag{I.3}$$

Equations (I.1) and (I.3) are solved for the derivative of  $h^*$

$$\left(\frac{\partial h^*}{\partial t}\right)_L = \Delta^* \Gamma^{h*} - \frac{1}{\Lambda^*} \left(\frac{\partial \Lambda^*}{\partial t}\right)_L \Gamma^{h*} - \Gamma^{h*} \left(\frac{\partial \Gamma^{r*}}{\partial t}\right)_L (\Gamma^{r*})^{-1}. \tag{I.4}$$

Since the volume of the representative unit cell is proportional to the cube of  $\Lambda^*$ ,

$$\frac{1}{\Lambda^*} \left(\frac{\partial \Lambda^*}{\partial t}\right)_L = -\frac{1}{3} \frac{1}{\rho^*} \left(\frac{\partial \rho^*}{\partial t}\right)_L = +\frac{1}{3} \nabla \cdot \mathbf{v}^*. \tag{I.5}$$

Here equation (3.1) is used. The last term on the right of equation (I.4) is determined for the special case in which all derivatives are first order in  $h^*$ . The matrix  $\Gamma^{h*}$  on the right side of equation (I.4) is approximated by the identity. Since  $\Gamma^{r*}$  is a rotation matrix,  $(\partial \Gamma^{r*} / \partial t)_L (\Gamma^{r*})^{-1}$  is antisymmetric. The left side of equation (I.4) is symmetric. Subtracting the transpose of equation (I.4) from equation (I.4) yields

$$\left(\frac{\partial \Gamma^{r*}}{\partial t}\right)_L (\Gamma^{r*})^{-1} = \frac{1}{2} (\Delta^* - \Delta^{*t}). \tag{I.6}$$

The superscript  $t$  denotes the transpose. Equations (I.5) and (I.6) are substituted into equation (I.4) and the result in terms of the individual elements of the matrices is equation (2.5).

### APPENDIX II

Equation (3.4) for the elastic stress tensor is derived from equation (2.7) using the equations obtained by deleting all dissipative terms from the kinematical equations, the momentum equations, and the energy equation. Equation (2.7) is differentiated

$$\left(\frac{\partial E^*}{\partial t}\right)_L = \frac{\partial E_g^*}{\partial \rho^*} \left(\frac{\partial \rho^*}{\partial t}\right)_L + 2C_t^{*2} \sum_{ij} h_{ij}^* \left(\frac{2h_{ij}^*}{\partial t}\right)_L. \tag{II.1}$$

The derivative of the specific entropy vanishes because there are no dissipative processes, and terms containing  $h_{ij}^{*2}$  times a derivative are neglected because they are third order in  $h^*$ . Equations (2.5), (2.8) and (3.1) are substituted into equation (II.1).

$$\left(\frac{\partial E^*}{\partial t}\right)_L = -\frac{P^*}{\rho^*} \nabla \cdot \mathbf{v}^* - 2C_t^{*2} \sum_{ij} h_{ij}^* (\nabla_i v_j^*). \tag{II.2}$$

The last term on the right of equation (II.2) depends on the symmetry and vanishing trace of  $h^*$ . The equivalence of equations (II.2) and (3.3) implies equation (3.4).

### APPENDIX III

First order terms in equation (2.7) together with equation (2.8) yield

$$E = \frac{P}{\rho^2} P' + TS'. \tag{III.1}$$

The vanishing of all elements of  $h$  is used to derive equation (III.1). Equation (III.1) is substituted into equation (3.8).

$$\frac{P}{\rho} \mathbf{v} \cdot \nabla \rho' + \rho T \mathbf{v} \cdot \nabla S' = -P \nabla \cdot \mathbf{v}' \tag{III.2}$$

Equations (3.6) and (III.2) imply the second term on the left of equation (III.2) vanishes. Equation (3.9) is obtained immediately because the basic flow must have non-vanishing temperature and density.

The density may be considered to be a function of pressure, specific entropy, and the independent elements of  $h^*$ . The first-order terms are independent of the elements of  $h'$  because  $h$  vanishes.

$$\rho' = \left( \frac{\partial \rho}{\partial P} \right)_S P' + \left( \frac{\partial \rho}{\partial S} \right)_P S'. \tag{III.3}$$

In fluid dynamics, the partial derivative of pressure with respect to density at constant specific entropy is the speed of sound [4, 5]. Equations (III.3) and (3.9) yield

$$\mathbf{v} \cdot \nabla \rho' = \frac{1}{C_s^2} \mathbf{v} \cdot \nabla P'. \tag{III.4}$$

Equations (3.6) and (III.4) yield equation (3.10).

### APPENDIX IV

Equation (3.4) is substituted into the right side of equation (3.17) and the result is

$$\begin{aligned} \sum_{ij} (\sigma_{ij}^* v_i^* - \sigma_{ij}^A v_i^A) n_j^* &= -(P^* \mathbf{v}^* - P^A \mathbf{v}^A) \cdot \mathbf{n}^* + 2\rho^* C_i^{*2} \sum_{ij} h_{ij}^* v_i n_j^* \\ &= -J^* \left( \frac{P^*}{\rho^*} - \frac{P^A}{\rho^A} \right) + 2\rho^* C_i^2 \sum_{ij} h_{ij}^1 v_i e_{sj}. \end{aligned} \tag{IV.1}$$

The second term is correct to first order. The specific enthalpy (in Mie-Grüneisen approximation)  $I^*$  simplifies equation (3.17)

$$I^* = E^* + \frac{P^*}{\rho^*} \tag{IV.2}$$

$$J^*(I^* + \frac{1}{2} v^{*2} - I^A - \frac{1}{2} v^{A2}) = 2\rho^* C_i^2 \sum_{ij} k_{ij}^1 v_i e_{sj}. \tag{IV.3}$$

The unperturbed part of the parenthesis on the left vanishes, and  $J^*$  may be replaced by  $J$ . The parenthesis is calculated to first order using thermodynamic identities.

$$\begin{aligned} I^* + \frac{1}{2} v^{*2} - I^A - \frac{1}{2} v^{A2} &= I' + \mathbf{v} \cdot \mathbf{v}' \\ &= \frac{1}{\rho} P' + T S' + \mathbf{v} \cdot \mathbf{v}'. \end{aligned} \tag{IV.4}$$

If equation (IV.4) is substituted into equation (IV.3), equation (3.21) is obtained.

Equation (III.3) may be substituted directly into equation (3.18). If the normal component of the unperturbed velocity, denoted by  $v \cdot e_s$  in equation (3.18), is replaced by  $(J/\rho)$ , equation (3.23) is obtained.

*(Received 31 August 1972; revised 8 January 1973)*

**Абстракт**—С теоретической точки зрения исследуется рефракция упруго-пластического удара, который падает при малых углах на поверхность раздела материала. Основное течение является многократной формой удара, которая описывает регулярное отражение в динамике жидкостей. Поправки к основному течению удовлетворяют уравнениям возмущения первого рода. Эти уравнения решаются асимптотически.